Published in final edited form as:
Nat Med. 2008 June ; 14(6): 648–655. doi:10.1038/nm1760.

The Ashwell receptor mitigates the lethal coagulopathy of sepsis

Prabhjit K Grewal[1], **Satoshi Uchiyama**[2], **David Ditto**[3], **Nissi Varki**[3], **Dzung T Le**[3], **Victor Nizet**[2,4], and **Jamey D Marth**[1]

[1] The Howard Hughes Medical Institute and Department of Cellular and Molecular Medicine, 9500 Gilman Drive, University of California, San Diego, La Jolla, California 92093, USA

[2] Department of Pediatrics, University of California, 9500 Gilman Drive, University of California, San Diego, La Jolla, California 92093, USA

[3] Department of Pathology, University of California, 9500 Gilman Drive, University of California, San Diego, La Jolla, California 92093, USA

[4] Skaggs School of Pharmacy and Pharmaceutical Sciences, 9500 Gilman Drive, University of California, San Diego, La Jolla, California 92093, USA

Abstract

The Ashwell receptor, the major lectin of hepatocytes, rapidly clears from blood circulation glycoproteins bearing glycan ligands that include galactose and *N*-acetylgalactosamine. This asialoglycoprotein receptor activity remains a key factor in the development and administration of glycoprotein pharmaceuticals, yet a biological purpose of the Ashwell receptor has remained elusive. We have identified endogenous ligands of the Ashwell receptor as glycoproteins and regulatory components in blood coagulation and thrombosis that include von Willebrand factor (vWF) and platelets. The Ashwell receptor normally modulates vWF homeostasis and is responsible for thrombocytopenia during systemic *Streptococcus pneumoniae* infection by eliminating platelets desialylated by the bacterium's neuraminidase. Hemostatic adaptation by the Ashwell receptor moderates the onset and severity of disseminated intravascular coagulation during sepsis and improves the probability of host survival.

The liver controls the removal of exogenously administered glycoproteins from circulation, as discovered over 35 years ago[1–4]. These classical investigations identified the first vertebrate lectin as a hepatic receptor for glycoproteins bearing glycan chains that lack sialic acid, termed asialoglycoproteins[5,6]. Today, the Ashwell receptor is known to be one of multiple lectins of the C-type lectin family that bind asialoglycoproteins, and its activity remains a fundamental consideration in the design of clinical treatments to provide therapeutic levels of glycoproteins in circulation[7,8]. Mammalian asialoglycoprotein receptors (ASGPRs) mediate the capture and endocytosis of a wide range of exogenously administered glycoproteins that have galactose or *N*-acetylgalactosamine residues at the termini of their glycan chains. More recent findings have indicated that some sialylated glycans are also ligands for the Ashwell receptor[9]. Localized to the vascular face of the hepatocyte cell surface, the Ashwell receptor is positioned to remove and degrade potentially deleterious circulating glycoproteins[6,10,11]. Nonetheless, the biological purpose of this lectin has remained an enigma. Endogenous ligands have not been identified, and the conservation of the Ashwell receptor throughout vertebrate evolution remains unexplained.

Correspondence should be addressed to J.D.M. (jmarth@ucsd.edu).

The Ashwell receptor is composed of type 2 transmembrane glycoproteins termed asialoglycoprotein receptor-1 (Asgr-1) and asialoglycoprotein receptor-2 (Asgr-2) that are encoded by distinct but closely linked genes, with variation in Asgr-2 structure due to RNA splicing[12–14]. Both *Asgr1* and *Asgr2* are highly conserved among mammalian species and may have originated from a single ancestral gene[15–17]. Although Asgr1 and Asgr2 are detectable in some extra-hepatic tissues, they are predominantly expressed in the liver and are often used as markers of hepatocytes. Oligomerization of the Asgr-1 and Asgr-2 glycoproteins has been observed in various cellular contexts, with these findings supporting the possibility that Ashwell receptors may exist as Asgr-1–Asgr-2 hetero-oligomers, Asgr-1 homotrimers and homotetramers, and Asgr-2 homodimers and homotetramers, perhaps thereby altering substrate selectivity, binding affinities and rates of endocytosis[18–24]. Notably, although mice deficient in either Asgr-1 or Asgr-2 show decreased clearance of exogenous desialylated glycoproteins, they do not accumulate endogenous asialoglycoproteins in the circulation, and they lack phenotypic abnormalities[25–27]. Because α2,3-linked sialic acid can mask underlying ASGPR ligands on glycoproteins, we suspected that reducing the expression of these sialic acid linkages *in vivo* among endogenous glycoproteins might unmask ligand identity and thereby facilitate investigations of Ashwell receptor function in biology and disease.

The ST3Gal family of sialyltransferases includes enzymes that add sialic acid in α2,3 linkage to galactose residues at the termini of *N*- and *O*-glycan chains and that can thereby mask endogenous ASGPR ligands. Thus, a genetic approach to disrupt sialyltransferase function in the mammalian germline might expose endogenous ligands for one or more lectins with asialoglycoprotein-binding activity, including the Ashwell receptor, the Kupffer cell receptor, the macrophage galactose receptors and the galectins. Indeed, when the *St3gal4*-encoded sialyltransferase (ST3Gal-IV) is limiting or absent, such ligands appear on a subset of regulatory and prothrombotic components of the mammalian blood coagulation system, including vWF and platelets[28]. ST3Gal-IV deficiency causes prolonged bleeding and coagulation times attributable to ASGPR-mediated clearance of these clotting factors from circulation[28]. These studies have revealed that endogenous ASGPR activity is poised to cause rapid hemostatic modulation in response to a reduced sialylation state of platelets, vWF and possibly other blood components. Here we investigate whether vWF and platelets may be endogenous ligands of the Ashwell receptor and whether they are subject to clearance during pathologic conditions of rapid desialylation, such as bloodstream infection with a microbe expressing sialidase (neuraminidase) activity.

RESULTS

Ashwell receptors govern vWF homeostasis

We observed localization of the vWF glycoprotein *in situ* primarily among liver endothelial cells, but also among hepatocytes; in which the majority of vWF colocalized with the Asgr-1 chain of the Ashwell receptor (Fig. 1a). In contrast, there was markedly less colocalization of hepatocyte vWF with Asgr-2 (Fig. 1b). In mice homozygous for null mutations in either *Asgr1* or *Asgr2* (refs. [25,29]), the other closely linked gene retained function, and the corresponding Asgr glycoprotein remained expressed (Fig. 1c). Furthermore, the absence of Asgr-1, but not of Asgr-2, reduced the total amount of vWF associated with hepatocytes, resulting in an increased percentage of the remaining vWF that colocalized with Asgr-2 (Fig. 1c).

Circulating plasma vWF abundance was increased 1.5-fold in mice lacking Asgr-1 in comparison either to mice lacking Asgr-2 or wild-type (WT) littermates (Fig. 1d). The elevated vWF in Asgr-1 deficiency was paralleled by an increased abundance of plasma factor VIII, a procoagulation factor that binds to and is stabilized by vWF in the circulation

(Fig. 1e). No changes in vWF or factor VIII were observed in Asgr-2–deficient mice, and factor IX, factor XI and factor XII were unaffected in mice with null mutations in either *Asgr1* or *Asgr2* (Fig. 1e). Elevated abundance of plasma vWF in Asgr-1–deficient mice correlated with increased vWF half-life in the circulation (Fig. 1f). Nonetheless, the elevation of vWF levels did not result in an increase in the frequency of asialo-vWF (data not shown). These findings reveal that the Ashwell receptor is normally engaged in the control of endogenous vWF clearance and homeostasis, implying a receptor-ligand relationship and suggesting a role in modulating blood coagulation and thrombosis.

Functional intersection of the Ashwell receptor and ST3Gal-IV

Mice lacking Asgr-1 had a reduced bleeding time compared to WT littermates, whereas their counterparts lacking Asgr-2 were unaffected (Fig. 1g). Because ASGPR-mediated clearance of vWF occurs in ST3Gal-IV sialyltransferase deficiency, we hypothesized that the Ashwell receptor and ST3Gal-IV may jointly control endogenous vWF homeostasis. We studied mice bred to lack ST3Gal-IV function as well either Asgr-1 or Asgr-2. Asialo-vWF was detected by the absence of sialic acid linkages at the termini of various glycan chains using plant-derived galactose binding lectins as previously described[28] and was the dominant vWF glycoform in circulation in all strains of mice lacking ST3Gal-IV function (data not shown). Notably, the diminished abundance and shortened half-life of plasma vWF due to ST3Gal-IV deficiency were restored to normal by the additional loss of Asgr-1, whereas, in contrast, loss of Asgr-2 did not result in such a rescue (Fig. 1h and data not shown). Moreover, Asgr-1 deficiency also corrected the prolonged bleeding and activated partial thromboplastin times in the absence of ST3Gal-IV, which is consistent with normalization of circulating vWF and consequently factor VIII abundance (Fig. 1h and data not shown).

Unexpectedly, mice lacking Asgr-2 and ST3Gal-IV, despite their vWF deficit, had a marked reduction in bleeding time compared to mice lacking only ST3Gal-IV (Fig. 1h). Because platelets that are deficient in sialic acid linkages (asialo-platelets) are also found in the circulation of mice lacking ST3Gal-IV function, with resultant thrombocytopenia (low platelet count) due to ASGPR-mediated clearance[28], we suspected that the Ashwell receptor might also control platelet homeostasis.

The Ashwell receptor in platelet homeostasis

Circulating platelet counts were unaffected in mice homozygous for either *Asgr1* or *Asgr2* mutation; however, the low platelet counts of mice with ST3Gal-IV deficiency were restored to normal in littermates that further lacked either Asgr-1 or Asgr-2 (Fig. 2a). Platelet volume, reticulated (newly formed) platelet abundance, and platelet half-life were also normalized (Fig. 2b–**d**). No alterations in red blood cell half-life occurred in parallel measurements (data not shown).

The liver is a major anatomic site of normal platelet clearance, and Kupffer cells, the resident macrophages of the liver, contribute to this clearance activity[30,31]. Hepatocytes are not generally considered to have a significant role. However, platelets have been observed within hepatocytes in some contexts, and the ability of hepatocytes to clear desialylated platelets has been recently reported in studies of platelet binding and internalization[32,33]. We observed that the majority of platelets in the livers of WT mice are normally associated with Kupffer cells (Fig. 2e). In ST3Gal-IV–deficient mice, despite an overall increase in platelet sequestration in the liver, there was a decrease in the percentage of platelets associated with Kupffer cells (Fig. 2e). In the acute setting of plasma transfusion, biotinylated asialo-platelets derived from ST3Gal-IV–deficient donors were more abundant in the livers of post-transfused wild-type recipients, and the majority were associated with hepatocytes, as compared to the abundance and localization of post-transfused biotinylated WT platelets

bearing normal abundance of sialic acid linkages (Fig. 2f). We conclude that ST3Gal-IV deficiency exposes endogenous glycan ligands on platelets that are recognized by the Ashwell receptor in an interaction that promotes asialo-platelet clearance by hepatocytes and leads to thrombocytopenia.

Bacterial sialidase activity and the Ashwell receptor

The location, high capacity and rapid kinetics of ligand clearance by the Ashwell receptor is consistent with its anticipation of a sudden and widespread alteration of endogenous glycoprotein structure within the circulatory system. Such conditions might arise after infection by pathogens that encode sialidase (neuraminidase) activity, such as *Streptococcus pneumoniae*, a leading cause of sepsis and the life-threatening thrombohemorrhagic disorder known as disseminated intravascular coagulation, manifested by rapid consumption of platelets and coagulation factors[34–36].

We administered a lethal dose of *S. pneumoniae* (isolate D39) to WT mice by intraperitoneal (i.p.) injection and monitored platelet glycosylation in mice with comparable bacterial counts in the blood before death. Circulating platelets were progressively desialylated during *S. pneumoniae* sepsis, as evidenced by an increase in galactose exposure (Fig. 3a). In contrast, loss of sialic acid from the surface of red blood cells was not detected. Infection of WT mice with an isogenic *nanA* mutant strain of *S. pneumoniae* lacking the sialidase enzyme NanA[37] (NanA$^-$) did not generate asialo-platelets in circulation (Fig. 3b). Bacteremia during the progression of sepsis after infection of WT mice with the *S. pneumoniae* NanA$^-$ isogenic mutant was similar to that seen with infection by the parental *S. pneumoniae* D39 strain (*S. pneumoniae* WT), in contrast to a previous finding in which an *S. pneumoniae* NanA$^-$ isolate failed to propagate in circulation[38]. Complementation of NanA activity in *trans* (NanA^T) restored platelet desialylation similar to that seen with *S. pneumoniae* WT (Fig. 3c). These studies identify the bacterial NanA neuraminidase as the sialidase responsible in sepsis for platelet desialylation.

The thrombocytopenia that occurs in sepsis is believed to reflect accelerated platelet consumption due to increased blood coagulation. Upon infection of WT mice with *S. pneumoniae* WT, thrombocytopenia developed before death, as expected (Fig. 3d). In contrast, when the same challenge was applied to Asgr-1–deficient mice, platelet levels were comparable to those in uninfected mice (Fig. 3d). Normal platelet counts were also present in WT mice infected with the *S. pneumoniae* NanA$^-$ mutant, whereas thrombocytopenia was again triggered when the *S. pneumoniae* NanA$^-$ mutant was complemented with the intact *nanA* gene (Fig. 3d). Consistent with these findings, platelet half-life decreased during *S. pneumoniae* WT infection of WT mice but was unaltered in mice lacking Asgr-1 after an identical challenge (Fig. 3e). The Ashwell receptor is not itself involved in controlling sialidase function, as the amount of platelet desialylation produced by *S. pneumoniae* NanA was identical in WT and Asgr-deficient hosts (data not shown). In addition, vWF was desialylated during *S. pneumoniae* WT infection at higher bacterial loads, and under these conditions there was evidence of increased clearance of asialo-vWF (Fig. 3f). Thus, during *S. pneumoniae* sepsis, the hepatic Ashwell receptor is responsible for the induction of thrombocytopenia in response to platelet desialylation by the bacterial NanA sialidase.

The Ashwell receptor reduces coagulopathy and increases survival

We suspected that the reduction of prothrombotic factors during *S. pneumoniae* sepsis might moderate the pathologic outcome in the host. Thus, we determined the time to death after *S. pneumoniae* WT infection. Mice retaining Ashwell receptor function survived considerably longer than littermates that were deficient in either Asgr-1 or Asgr-2; whereas those lacking Asgr-1 succumbed most rapidly (Fig. 4a). Of note, WT mice rendered septic by the *S.*

pneumoniae NanA^{-} mutant also died sooner than those infected with *S. pneumoniae* WT, mirroring the decreased survival time associated with Asgr-1 deficiency, whereas complementation of the NanA^{-} mutant restored survival times to similar values as observed with *S. pneumoniae* WT infection (Fig. 4b). We suspected that Ashwell receptor function may moderate the severity of disseminated intravascular coagulation during sepsis. When mice had comparable bacteremia, and on average 12 h before their expected time of death, we undertook histopathological analysis of organs and tissues. Hemorrhage of the spleen was observed in all mice lacking Asgr-1 but was absent from WT littermates (Fig. 4c). In addition, vascular occlusion and fibrin deposition were markedly elevated in the kidney in the absence of Asgr-1 (Fig. 4d). Further signs of severe disseminated intravascular coagulation were observed in the liver of Asgr-1–deficient mice, with increased fibrin deposition in sinusoids and more severe venous thromboembolic occlusion (Fig. 4e). These pathological findings in Asgr-1–deficient mice were coincident with an increase in hepatocyte cell death (Fig. 4e). A similar increase in the severity of disseminated intravascular coagulation, including fibrin deposition, thrombosis and hemorrhage portending multi-organ failure, was also observed in WT mice rendered septic by the *S. pneumoniae* NanA^{-} mutant (Fig. 5). Notably, in a lower-dose challenge model using *S. pneumoniae* WT, all Asgr-1–deficient mice succumbed to infection, compared to a 37% survival rate of WT hosts (Fig. 6). The Ashwell receptor thus impedes the pathogenesis of disseminated intravascular coagulation and improves the probability of host survival in *S. pneumoniae* sepsis.

DISCUSSION

S. pneumoniae is a preeminent human pathogen and one of the leading causes of death worldwide, especially in infants and young children[39,40]. Sepsis caused by *S. pneumoniae* infection can trigger disseminated intravascular coagulation (DIC), a life-threatening complication involving the consumption of procoagulants and platelets with the deposition of intravascular fibrin throughout the body, resulting in multi-organ failure[35,36,40]. This thrombohemorrhagic pathology is lethal among a significant fraction of patients with severe septicemia and in intensive care. Our findings indicate that the marked thrombocytopenia closely associated with *S. pneumoniae* sepsis is neither mediated by the pathogen *per se* nor due to platelet consumption in DIC. Instead, thrombocytopenia is the result of Ashwell receptor–dependent clearance of platelets that are first desialylated by the NanA sialidase of the pathogen. Host glycoprotein remodeling by *S. pneumoniae* NanA retards the onset of severe hematologic changes that are indicative of acute DIC. Consequently, a subset of normal mice can survive challenge with limiting doses of *S. pneumoniae* that are lethal to littermates deficient in Ashwell receptor function.

Both the Asgr-1 and Asgr-2 chains of the Ashwell receptor are required for asialo-platelet clearance, and a deficiency of either leads to a shortened survival time in *S. pneumoniae* sepsis. The time to death upon challenge with a lethal dose of *S. pneumoniae* WT was prolonged to a lesser extent by Asgr-2 deficiency as compared to Asgr-1 deficiency. This suggests that asialo-vWF clearance, mediated by Asgr-1 but not Asgr-2, may be important for the relative efficacy of Asgr-1 deficiency in prolonging survival. However, an increased protective effect of Asgr-1 deficiency as compared to Asgr-2 deficiency against severe DIC and morbidity is not yet clearly established, and additional studies are needed to determine the precise lethal dose range of *S. pneumoniae* in mice deficient in either Asgr-1 or Asgr-2.

The Asgr-1 chain of the Ashwell receptor normally participates in plasma vWF homeostasis independently of sialylation and sepsis. Although we found that asialo-vWF is rapidly removed from circulation by Asgr-1, asialo-vWF accumulation did not occur in Asgr-1–deficient mice. This may be explained by the previously documented ability of the Ashwell

receptor to bind sialo- as well as asialo-glycoproteins as potential endogenous ligands[9]. We observed increased colocalization of vWF with Asgr-2 in Asgr-1–deficient mice, even after adjustment for reduced hepatocyte vWF abundance in these mice, consistent with the possibility that there may be some compensation by Asgr-2. Nevertheless, plasma vWF abundance is not altered by Asgr-2 deficiency. There seems to be less interdependence and overlap between Asgr-1 and Asgr-2 function than might be expected, and we observed that either chain of the Ashwell receptor can be expressed in the absence of the other *in vivo*. Our findings reveal that vWF and platelets are endogenous ligands of the Ashwell receptor, implying that hepatocytes are involved in the clearance of these coagulation factors from the circulation, which is an unexpected biological activity for this cell type.

Respiratory pathogens other than *S. pneumoniae*, including *Haemophilus influenzae*, *Pseudomonas aeruginosa* and influenza virus, also express one or more sialidases that target host glycoconjugates to reveal cellular receptors for mucosal adherence or cell penetration[41–44]. Not all pathogens that evoke DIC express sialidase activity, however; thus, for these pathogens, the Ashwell receptor would not be expected to modulate pathogenicity by asialoglycoprotein clearance. All *S. pneumoniae* strains isolated in nature express the NanA sialidase as a virulence factor that promotes mucosal colonization[45,46]. However, we find that NanA also reduces the severity of DIC, revealing an antivirulence activity of NanA that may serve the *S. pneumoniae* pathogen by lessening the likelihood of host mortality. NanA expressed by *S. pneumoniae* during sepsis removes a subset of α2,3-linked sialic acids but does not appear to remove this sialic acid linkage from the core 1 *O*-glycan structure and thus does not expose the Thomsen-Friedenreich antigen, as indicated by unaltered peanut agglutinin lectin binding on either platelets or red blood cells. Although different sialic acid linkages often have unique functions[47], loss of sialic acids in general can reduce the negative charge at the platelet surface and may in some cases alter their aggregation properties and contribute to disease[48]. We hypothesize that the effect of such changes may be exaggerated by aspects of the acute cellular pathophysiology of sepsis, including endothelial dysfunction and leukocyte activation. Of note, the asialo-platelets that accumulate in uninfected ST3Gal-IV deficient mice did not show altered activation profiles or responses (P.K.G., S.U., D.D., N.V., D.T.L. *et al.*, unpublished data), and the substantial elevation of circulating asialo-platelet concentration in mice lacking ST3Gal-IV and either Asgr-1 or Asgr-2 was not associated with obvious pathologic changes.

Ashwell receptor expression in hepatocytes is induced rapidly upon birth; the fetus lacks this mechanism of removing circulating glycoproteins[49]. As a post-partum glycoprotein and platelet clearance system, the Ashwell receptor may have had a major evolutionary role in the outcome of infection by *S. pneumoniae* and perhaps other systemic pathogens. Moreover, the changing ligand specificity of Ashwell receptors in phylogeny[50,51] reflects increasing glycan complexity in the host and perhaps mirrors the evolving infectious nature of various pathogens. It is unclear whether the Ashwell receptor provides a selective advantage among vertebrates in the absence of infection. ST3Gal-IV and perhaps other sialyltransferases may be regulated in some circumstances to desialylate endogenous glycoproteins and thereby engage Ashwell receptor clearance activity. Such regulation has yet to be documented, however, and the normal turnover of endogenous circulating glycoproteins has not been linked to ASGPR activity[10]. Nevertheless, endogenous sialidases in vertebrates may be involved in some clinical and pathogenic contexts. For example, loss of both sialic acid and galactose from the surface of chilled platelets prepared for transfusion may reflect extracellular glycosidase activities that thereby provoke rapid platelet clearance via binding of exposed *N*-acetylglucosamine to $\alpha_M\beta_2$ integrin on liver-resident Kupffer cells[31].

The Ashwell receptor provides an adaptive response to *S. pneumoniae* infection by detecting the byproducts of NanA sialidase activity on host blood factors and removing these prothrombotic components from circulation, preventing them from promoting the lethal complications of DIC. These results reveal a critical hemostatic role for hepatocytes in the acute pathology of sepsis and show that the Ashwell receptor is a key factor in determining host survival. Similar hemostatic modulation may be induced by treatments that likewise deplete platelet and prothrombotic coagulation factor abundance and function. Exogenously administered sialidase is, for example, capable of desialylating platelets and inducing thrombocytopenia[52]. Methods to engage and enhance the Ashwell receptor system may provide a new therapeutic opportunity for impeding the development of DIC in life-threatening systemic infections.

METHODS

Mice

Asgr1 mutant mice (ref. [29]) were kindly provided by B. Sauer (Stowers Institute for Medical Research, Kansas City, Missouri). We purchased *Asgr2* mutant mice from The Jackson Laboratory, stock 002387 (ref. [25]). Mice bearing a mutation in the gene encoding ST3Gal-IV (*St3gal4*) have been previously described[28]. We generated mice homozygous for multiple mutant alleles from parental mice with *St3gal4* $^{\Delta/\Delta}$*Asgr1*$^{+-}$ or *St3gal4* $^{\Delta/\Delta}$*Asgr2* $^{+-}$ genotypes. We observed no phenotypic differences between males and females. Prior to experimentation, we backcrossed all strains of mice to C57BL/6NHsd mates for at least eight generations and provided sterile pellet food and water *ad libitum*. We used littermates aged 8–13 weeks in all studies presented. All animal use and procedures were approved by the Institutional Animal Care and Use Committee of the University of California, San Diego.

Histology

For histological staining, we used tissues fixed in 10% buffered formalin, trimmed, processed, embedded in paraffin and sectioned at a width of 5 μm. For immunofluorescence studies, we stained glass slides bearing 5-μm sections of frozen embedded liver tissue (in OCT medium; Sakura Finetek). Antibodies included FITC-conjugated sheep antibody to human vWF (Abcam), goat antibody to mouse ASGPR1 and goat antibody to human ASGPR2 (Santa Cruz Biotech), phycoerythrin (PE)-conjugated rat antibody to mouse CD41 (BD Pharmingen), Alexa Fluor 647–phalloidin to detect actin (Invitrogen), FITC-conjugated rat antibody to mouse CD68 (Serotec) and Texas Red–conjugated antibody to goat IgG secondary antibodies (Jackson Immuno-Research Labs). We performed all primary antibody incubations (1:200) at 4 °C overnight and secondary antibody incubations (1:1,000) at 22 °C for 1 h and then mounted the slides with aqueous gel mount (Biomeda). We obtained images by fluorescence deconvolution microscopy with a DeltaVision Restoration microscope (Applied Precision) and analyzed them with DeltaVision SoftWorx (Version 2.50). We acquired and processed images identically within all comparative studies. Images were quantified for immunofluorescence signal, colocalization or both with MetaMorph software (Universal Imaging).

At 24–48 h after infection with *S. pneumoniae*, we collected organs for histopathological and morphometric examination. Organs from mice determined to have equivalent amounts of bacteria in the blood were immersion-fixed, embedded in paraffin, sectioned and stained with H&E (Surgipath) using standard histological techniques. We prepared the Fraser-Lendrum stain (Sigma) and used it to identify fibrin deposition (red) and red blood cells (yellow or orange). Two investigators blind to the experimental group microscopically examined the stained tissue sections for semiquantitative analysis. We scored 20 randomly

selected fields of view for fibrin deposits in capillaries. We counted 100 central and portal veins from random liver sections at three tissue depths and scored them as unclotted owing to the presence of red blood cells, clotted owing to visible fibrin thrombi or empty owing to upstream thrombi. We scored 20 randomly selected fields of view for fibrin deposits in sinusoids and used 30 randomly selected fields of view to assess pyknotic bodies and hepatocyte necrosis.

Hematology

We anesthetized mice by a mixture of 3% isoflurane with oxygen in an induction chamber maintained with a nose cone outside of the induction chamber. We transected tails of mice with a sterile razor blade 2 mm from the tip, collected whole blood (100 μl) in EDTA-containing polypropylene microtubes (Becton Dickinson) to ensure proper anticoagulation and kept the tubes at 22 °C until we could analyze them (within 4 h). We acquired blood cell counts with leukocyte differentials and platelet counts in duplicate on a Hemavet 850FS Multi Species Hematology System (Drew Scientific) programmed with mouse hematology settings. We prepared a whole-blood smear from each sample and Wright stained it for manual viewing. We performed coagulation factor analyses and clotting time assays as previously described[28].

von Willebrand factor analysis

We used vWF antibody and lectin binding assays to determine vWF glycosylation and glycoprotein abundance as previously described[28]. We determined vWF half-life after *ex vivo* biotinylation also as previously described[28].

Platelet measurements

We collected whole blood from retro-orbital or tail bleeds into EDTA-Vacutainer tubes (Becton Dickinson) and diluted it 1:30 in Tyrode's buffer (150 mM NaCl, 5 mM KCl, 1 mM $MgSO_4$, 10 mM HEPES, pH 7.4) before staining for flow cytometric analyses to determine glycosylation status[28], circulating platelet half-life or percentage of reticulated platelets. We performed all platelet analyses at 22 °C. We determined platelet half-lives after *in vivo* biotinylation by infusion of *N*-hydroxysuccinimide–biotin (Pierce). We injected 10 mg of *N*-hydroxysuccinimide–biotin (dissolved in DMSO, diluted to 500 μl volume in PBS) per kg of mouse body weight into the lateral tail vein. We collected 30 μl of whole blood by tail bleed from anesthetized mice at 24-h intervals as indicated in Figures 2 and 3 for analysis by flow cytometry; time 0 measurements were determined 1 h after biotin injection. We determined the percentage of biotinylated cells by flow cytometric measurements of light scatter and detection by binding of PE-conjugated streptavidin and FITC-conjugated antibody to CD41 (platelets) and APC-conjugated antibody to ter199 (red blood cells) (BD Pharmingen). Biotinylation efficiency varied between 80–95%. Levels of biotinylated platelets and red blood cells in circulation were based on measurements at time 0, denoted as 100%.

We calculated the percentage of reticulated platelets using RNA staining methods with Thiazole Orange (TO; Sigma). We diluted 2 μl of whole blood 1:30 in Tyrode's buffer and incubated it with 0.1 μg of PE-conjugated CD41-specific antibody at a final concentration of 1 μg/ml TO in PBS (stock of 1 mg/ml dissolved in methanol) for 10 min in the dark at 22 °C. We collected and analyzed flow cytometric data on 10,000 platelets. We confirmed identification of TO-positive platelets with RNase-pretreated whole blood.

Streptococcus pneumoniae infection

Wild-type *S. pneumoniae* serotype 2 strain D39 and its isogenic $NanA^-$ mutant[35] were kindly provided by T. Mitchell (University of Glasgow) and were grown in Todd-Hewitt

broth (Acumedia) with 2% yeast extract. After overnight incubation at 37 °C and 5% CO_2, we re-inoculated bacteria into fresh media, cultured them to mid-logarithmic growth phase (A_{600} = 0.4), centrifuged them at 1,500*g* for 5 min, washed them once and resuspended them in PBS. We performed infections as follows unless otherwise stated. We infected mice weighing 18–20 g with a dose of 2×10^5 colony-forming units (CFU) of bacteria in 100 μl by i.p. injection. At 24-h intervals after injection, we collected blood to enumerate bacterial CFU in circulation and to measure hematologic parameters as we monitored the time to death. Unless otherwise indicated, those mice with equivalent bacteremia (between 1×10^4 CFU/ml and 1×10^6CFU/ml at 24 h after infection followed by an increase to between 1×10^6 CFU/ml and 1×10^8 CFU/ml at 48 h after infection) were studied further. For platelet half-life determination, we injected mice with biotin 1 h before *S. pneumoniae* infection.

We generated the *S. pneumoniae* $NanA^T$ strain (expressing neuraminidase in *trans*) from the isogenic *S. pneumoniae* D39 NanA mutant strain transformed with a PDC123 plasmid containing the *S. pneumoniae nanA* gene. An overnight culture of *S. pneumoniae* grown in brain heart infusion medium (Fluka) was re-inoculated into fresh media with 1 mM $CaCl_2$. When the cultures had reached A_{600} = 0.1, we added competent stimulate peptide-1 (CSP-1) to a final concentration of 100 ng/ml before further incubation at 37 °C for 15 min. We added 100 ng plasmid PDC123 containing the *nanA* gene to this culture before plating it on a chloramphenicol-selective Todd-Hewitt broth plus 2% yeast extract (Becton Dickinson) plate for growth at 37 °C with 5% CO_2 overnight for positive colony selection.

Statistical analyses

All data are presented as the means ± s.e.m. unless otherwise indicated. We analyzed numeric data for statistical significance using Student's unpaired *t*-test with Prism software (GraphPad). We considered *P* values of less than 0.05 as statistically significant. Degrees of statistical significance are presented as ***$P < 0.001$, **$P < 0.01$ or *$P < 0.05$.

Acknowledgments

We thank L. Brown and Q. Chen for technical assistance with some of the experiments. Assistance with fluorescent microscopy was obtained from the University of California, San Diego Cancer Center Digital Imaging Shared Resource team directed by J. Feramisco. Mice with the germline mutation of the Asgr-1 hepatocyte asialoglycoprotein receptor were kindly provided by B. Sauer (Stowers Institute for Medical Research, Kansas City, Missouri). Wild-type *S. pneumoniae* serotype 2 strain D39 and its isogenic $NanA^-$ mutant were kindly provided by T. Mitchell (University of Glasgow). This research was funded by US National Institutes of Health grants HL-57345 to J.D.M., D.T.L. and N.V. and AI-051796 to V.N. and an American Heart Association Established Investigator Award to V.N. The Howard Hughes Medical Institute provides support to J.D.M.

References

1. van den Hamer CJA, Morell AG, Scheinberg IH, Hickman J, Ashwell G. Galactosyl residues in the clearance of ceruloplasmin from the circulation. J Biol Chem 1970;245:4397–4402. [PubMed: 4322435]
2. Morell AG, Gregoriadis G, Scheinberg IH, Hickman J, Ashwell G. The role of sialic acid in determining the survival of glycoproteins in the circulation. J Biol Chem 1971;246:1461–1467. [PubMed: 5545089]
3. Ashwell G, Morell A. The role of surface carbohydrates in the hepatic recognition and transport of circulating glycoproteins. Adv Enzymol 1974;41:99–128. [PubMed: 4609051]
4. Hudgin RL, Pricer WE Jr, Ashwell G, Stockert RJ, Morell AG. The isolation and properties of a rabbit liver binding protein specific for asialoglycoproteins. J Biol Chem 1974;249:5536–5543. [PubMed: 4370480]
5. Ashwell G, Kawasaki T. A protein from mammalian liver that specifically binds galactose-terminated glycoproteins. Methods Enzymol 1978;50:287–288. [PubMed: 661580]

6. Ashwell G, Harford J. Carbohydrate-specific receptors of the liver. Annu Rev Biochem 1982;51:531–534. [PubMed: 6287920]
7. Stockert RJ. The asialoglycoprotein receptor: relationships between structure, function, and expression. Physiol Rev 1995;75:591–609. [PubMed: 7624395]
8. Drickamer K. C-type lectin–like domains. Curr Opin Struct Biol 1999;9:585–590. [PubMed: 10508765]
9. Park EI, Mi Y, Unverzagt C, Gabius HJ, Baenziger JU. The asialoglycoprotein receptor clears glycoconjugates terminating with sialic acid α-2,6GalNAc. Proc Natl Acad Sci USA 2005;102:17125–17129. [PubMed: 16286643]
10. Weigel PH. Galactosyl and *N*-acetylgalactosaminyl homeostasis: a function for mammalian asialoglycoprotein receptors. Bioessays 1994;16:519–524. [PubMed: 7945281]
11. Wahrenbrock MG, Varki A. Multiple hepatic receptors cooperate to eliminate secretory mucins aberrantly entering the bloodstream: Are circulating cancer mucins the “tip of the iceberg”? Cancer Res 2006;66:2433–2441. [PubMed: 16489050]
12. Drickamer K, Mamon JF, Binns G, Leung JO. Primary structure of the rat liver asialoglycoprotein receptor. Structural evidence for multiple polypeptide species. J Biol Chem 1984;259:770–778. [PubMed: 6319386]
13. Halberg DF, et al. Major and minor forms of the rat liver asialoglycoprotein receptor are independent galactose-binding proteins. Primary structure and glycosylation heterogeneity of minor receptor forms. J Biol Chem 1987;262:9828–9838. [PubMed: 3597443]
14. Paietta E, Stockert RJ, Racevskis J. Alternatively spliced variants of the human hepatic asialoglycoprotein receptor, H2, differ in cellular trafficking and regulation of phosphorylation. J Biol Chem 1992;267:11078–11084. [PubMed: 1597447]
15. Spiess M, Lodish HF. Sequence of a second human asialoglycoprotein receptor: conservation of two receptor genes during evolution. Proc Natl Acad Sci USA 1985;82:6465–6469. [PubMed: 3863106]
16. Hong W, Le AV, Doyle D. Identification and characterization of a murine receptor for galactose-terminated glycoproteins. Hepatology 1988;8:553–558. [PubMed: 3371871]
17. Takezawa R, Shinzawa K, Watanabe Y, Akaike T. Determination of mouse major asialoglycoprotein receptor cDNA sequence. Biochim Biophys Acta 1993;1172:220–222. [PubMed: 8439566]
18. Hardy MR, Townsend RR, Parkhurst SM, Lee YC. Different modes of ligand binding to the hepatic galactose/*N*-acetylgalactosamine lectin on the surface of rabbit hepatocytes. Biochemistry 1985;24:22–28. [PubMed: 3994969]
19. Braiterman LT, et al. The major subunit of the rat asialoglycoprotein receptor can function alone as a receptor. J Biol Chem 1989;264:1682–1688. [PubMed: 2643601]
20. Henis YI, Katzir Z, Shia MA, Lodish HF. Oligomeric structure of the human asialoglycoprotein receptor: nature and stoichiometry of mutual complexes containing H1 and H2 polypeptides assessed by fluorescence photobleaching recovery. J Cell Biol 1990;111:1409–1418. [PubMed: 2211817]
21. Bider MD, Wahlberg JM, Kammerer RA, Spiess M. The oligomerization domain of the asialoglycoprotein receptor preferentially forms 2:2 heterotetramers in vitro. J Biol Chem 1996;271:31996–32001. [PubMed: 8943247]
22. Ruiz NI, Drickamer K. Differential ligand binding by two subunits of the rat liver asialoglycoprotein receptor. Glycobiology 1996;6:551–559. [PubMed: 8877376]
23. Saxena A, Yik JHN, Weigel PH. H2, the minor subunit of the human asialoglycoprotein receptor, trafficks intracellularly and forms homo-oligomers, but does not bind asialo-orosomucoid. J Biol Chem 2002;277:35297–35304. [PubMed: 12089159]
24. Weigel PH, Yik JHN. Glycans as endocytosis signals: the cases of the asialo-glycoprotein and hyaluronan/chondroitin sulfate receptors. Biochim Biophys Acta 2002;1572:341–363. [PubMed: 12223279]
25. Ishibashi S, Hammer RE, Herz J. Asialoglycoprotein receptor deficiency in mice lacking the minor receptor subunit. J Biol Chem 1994;269:27803–27806. [PubMed: 7961705]

26. Braun JR, Willnow TE, Ishibashi S, Ashwell G, Herz J. The major subunit of the asialoglycoprotein receptor is expressed on the hepatocellular surface in mice lacking the minor receptor. J Biol Chem 1996;271:21160–21166. [PubMed: 8702886]
27. Tozawa R, et al. Asialoglycoprotein receptor deficiency in mice lacking the major receptor subunit. Its obligate requirement for the stable expression of oligomeric receptor. J Biol Chem 2001;276:12624–12628. [PubMed: 11278827]
28. Ellies LG, et al. Sialyltransferase ST3Gal-IV operates as a dominant modifier of hemostasis by concealing asialoglycoprotein receptor ligands. Proc Natl Acad Sci USA 2002;99:10042–10047. [PubMed: 12097641]
29. Soukharev S, Miller JL, Sauer B. Segmental genomic replacement in embryonic stem cells by double lox targeting. Nucleic Acids Res 1999;27:e21. [PubMed: 10471751]
30. Stratton JR, Ballem PJ, Gernsheimer T, Cerqueira M, Slichter SJ. Platelet destruction in autoimmune thrombocytopenic purpura: kinetcs and clearance of indium-111–labeled autologous platelets. J Nucl Med 1989;30:629–637. [PubMed: 2497234]
31. Hoffmeister KM, et al. The clearance mechanism of chilled platelets. Cell 2003;112:87–97. [PubMed: 12526796]
32. Nakamura M, Shibazaki M, Nitta Y, Endo Y. Translocation of platelets into Disse spaces and their entry into hepatocytes in response to lipopolysaccharides, interleukin-1 and tumour necrosis factor: the role of Kupffer cells. J Hepatol 1998;28:991–999. [PubMed: 9672175]
33. Rumjantseva V, Josefsson EC, Wandall H, Hartwig JH, Stossel TP. Hepatocytes ingest long term refrigerated platelets: A novel platelet clearance mechanism. Blood (ASH Annual Meeting Abstracts) 2006;108:1523.
34. Camara M, Boulnois GJ, Andrew PW, Mitchell TJ. A neuraminidase from *Streptococcus pneumoniae* has the features of a surface protein. Infect Immun 1994;62:3688–3695. [PubMed: 8063384]
35. Bryant AE. Biology and pathogenesis of thrombosis and procoagulant activity in invasive infections caused by Group A streptococci and *Clostridium perfringens*. Clin Microbiol Rev 2003;16:451–462. [PubMed: 12857777]
36. Franchini M, Lippi G, Manzato F. Recent acquisitions in the pathophysiology, diagnosis and treatment of disseminated intravascular coagulation. Thromb J 2006;4:4. [PubMed: 16504043]
37. Winter AJ, et al. A role for pneumolysin but not neuraminidase in the hearing loss and cochlear damage induced by experimental pneumococcal meningitis in guinea pigs. Infect Immun 1997;65:4411–4418. [PubMed: 9353013]
38. Manco S, et al. Pneumococcal neuraminidases A and B both have essential roles during infection of the respiratory tract and sepsis. Infect Immun 2006;74:4014–4020. [PubMed: 16790774]
39. World Health Organization. Wkly Epidemiol Rec 2003;78:97–120. [PubMed: 12723281]
40. Remick DG. Pathophysiology of sepsis. Am J Pathol 2007;170:1435–1444. [PubMed: 17456750]
41. Roggentin P, Schauer R, Hoyer LL, Vimr ER. The sialidase superfamily and its spread by horizontal gene transfer. Mol Microbiol 1993;9:915–921. [PubMed: 7934919]
42. Paton JC, Andrew PW, Boulnois GJ, Mitchell TJ. Molecular analysis of the pathogenicity of *Streptococcus pneumoniae*: the role of pneumococcal proteins. Annu Rev Microbiol 1993;47:89–115. [PubMed: 7903033]
43. Suzuki Y. Sialobiology of influenza: molecular mechanism of host range variation of influenza viruses. Biol Pharm Bull 2005;28:399–408. [PubMed: 15744059]
44. Soong G, et al. Bacterial neuraminidase facilitates mucosal infection by participating in biofilm production. J Clin Invest 2006;116:2297–2305. [PubMed: 16862214]
45. Tong HH, Liu X, Chen Y, James M, Demaria T. Effect of neuraminidase on receptor-mediated adherence of *Streptococcus pneumoniae* to chinchilla tracheal epithelium. Acta Otolaryngol (Stockh) 2002;122:413–419. [PubMed: 12125999]
46. Shakhnovich EA, King SJ, Weiser JN. Neuraminidase expressed by *Streptococcus pneumoniae* desialylates the lipopolysaccharide of *Neisseria meningitidis* and *Haemophilus influenzae*: a paradigm for interbacterial competition among pathogens of the human respiratory tract. Infect Immun 2002;70:7161–7164. [PubMed: 12438402]

47. Ohtsubo K, Marth JD. Glycosylation in cellular mechanisms of health and disease. Cell 2006;126:855–867. [PubMed: 16959566]

48. Mandic R, Opper C, Krappe J, Wesemann W. Platelet sialic acid as a potential pathogenic factor in coronary heart disease. Thromb Res 2002;106:137–141. [PubMed: 12182913]

49. Zalik SE. On the possible role of endogenous lectins in early animal development. Anat Embryol (Berl) 1991;183:521–536. [PubMed: 1897740]

50. Park EI, Baenziger JU. Closely related mammals have distinct asialoglycoprotein receptor carbohydrate specificities. J Biol Chem 2004;279:40954–40959. [PubMed: 15262963]

51. Rice KG, Thomas VH, Yang Y. Probing the binding specificity of C-type lectins *in vivo*. Methods Enzymol 2003;363:90–104. [PubMed: 14579569]

52. Tribulatti MV, Mucci J, Van Rooijen N, Leguizamon MS, Campetella O. The trans-sialidase from *Trypanosoma cruzi* induces thrombocytopenia during acute Chagas' disease by reducing the platelet sialic acid contents. Infect Immun 2005;73:201–207. [PubMed: 15618155]

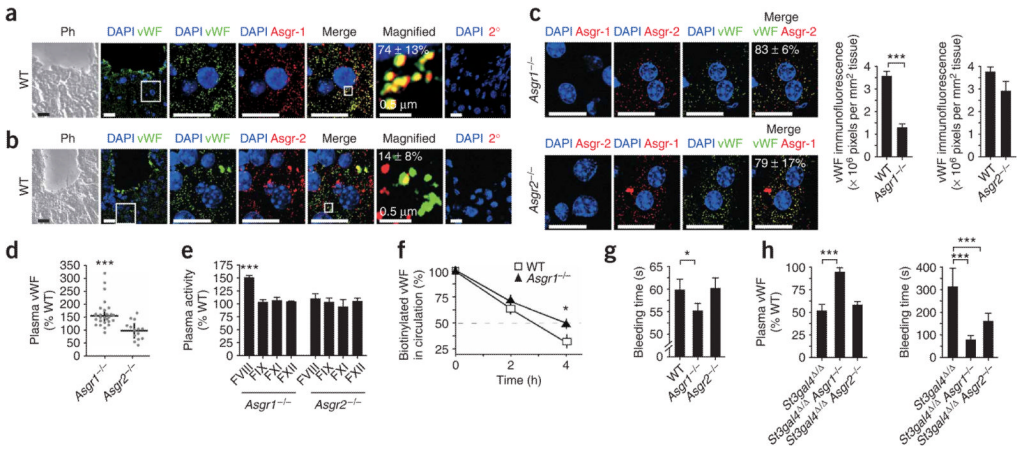

Figure 1.

Ashwell receptors of hepatocytes modulate vWF homeostasis and blood coagulation. (**a**–**c**) Liver sections from 8-week-old WT C57BL/6NHsd and Asgr-deficient mice imaged by phase-contrast (Ph) and fluorescent deconvolution microscopy using antibodies to vWF (green) and Asgpr-1 or Asgr-2 (red); DNA is stained by DAPI (blue). The percentage of vWF colocalized (yellow) with Asgr-1 (**a**) or Asgr-2 (**b**) in WT hepatocytes is indicated. Magnified views of the boxed regions are shown. Staining with Texas Red–conjugated secondary antibody to goat IgG (2°) alone is also shown. vWF abundance in Asgr-1–deficient hepatocytes compared to WT or Asgr-2–deficient hepatocytes is quantified (**c**). The percentage of vWF colocalized in Asgr-1–deficient or Asgr-2–deficient hepatocytes is indicated. The micrographs shown are representative of ten fields of view obtained from three mice of each genotype. All scale bars denote 5 μm unless otherwise indicated. (**d**) Plasma vWF abundance in mice lacking either Asgr-1 or Asgr-2. Horizontal bars indicate median vWF abundance, and vertical bars denote the interquartile range. (**e**) Coagulation factor measurements in mice lacking either Asgr-1 or Asgr-2 compared with WT littermates, ***$P < 0.001$. (**f**) Half-life of biotinylated plasma vWF from WT mice transfused into either WT or Asgr-1–deficient recipients. Plots represent data from eight WT and nine Asgr-1–deficient recipients. (**g**,**h**) Bleeding times (**g**) and bleeding times and plasma vWF abundance (**h**) in mice of the indicated genotypes. Mice homozygous for a null (deletion) mutation in the *St3gal4* gene are denoted as $St3gal4^{\Delta/\Delta}$. Histograms include data from 20–25 mice of each genotype. All values are means ± s.e.m.; ***$P < 0.001$; *$P < 0.05$.

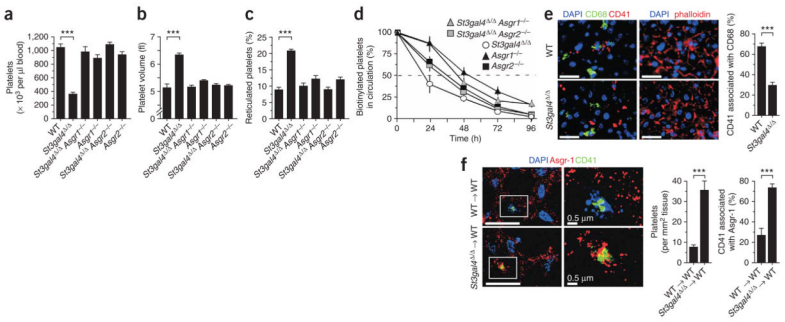

Figure 2.

The Ashwell receptor and the ST3Gal-IV sialyltransferase participate in platelet clearance. (**a**–**c**) Platelet abundance (**a**), mean platelet volume (**b**), and reticulated platelet frequencies (**c**) in mice of indicated genotypes. Histograms include data from 20–25 mice of each genotype. (**d**) Platelet half-life analyses in mice of indicated genotypes. Each curve includes data from six mice. Three separate experiments were performed. (**e**) Platelet antigens (CD41, left images) were detected in perfused liver sections of WT and *St3gal4*$^{\Delta/\Delta}$ mice, and hepatocytes were further visualized with DAPI and the actin-binding protein phalloidin (right images). Kupffer cells were detected by antibodies to CD68 (green). The images shown are representative of multiple fields of view from three mice of each genotype, comprising a total of 200 separate CD41 signals. (**f**) Sections of perfused liver were analyzed from WT recipients of biotinylated platelet-rich plasma from donors of the indicated genotypes to detect platelets (CD41, green) and Asgr-1 (red). Images are representative of multiple fields of view from three mice of each genotype, comprising a total of 46 separate CD41 signals. Scale bars denote 5 μm unless otherwise indicated. ***$P < 0.001$. All values are means ± s.e.m.

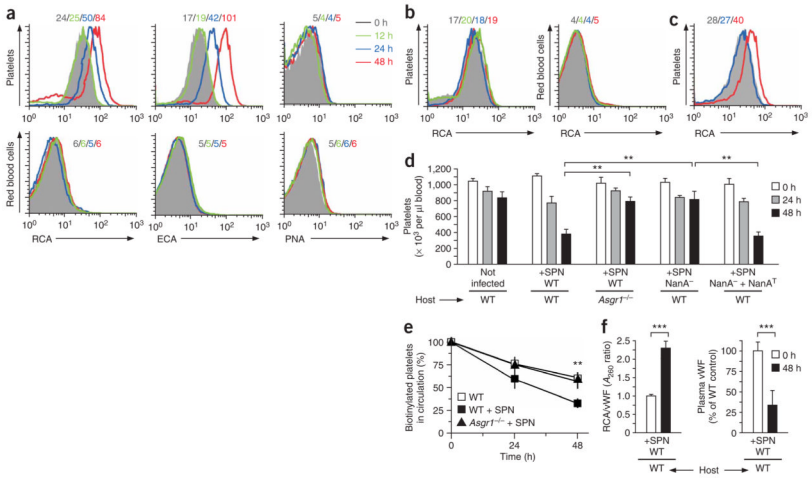

Figure 3.

Thrombocytopenia caused by NanA-dependent platelet desialylation and Ashwell receptor function in *S. pneumoniae* infection. (**a**) Asialoglycoproteins were detected by *Ricinus communis* agglutinin (RCA) and *Erythrina cristagalli* agglutinin (ECA) lectin binding at the indicated times after infection with *S. pneumoniae* strain D39 (*S. pneumoniae* WT). PNA lectin binding was used to detect the Thomsen Friedenrich antigen. Mean fluorescence is enumerated at the indicated times after infection. (**b**) Detection of asialoglycoproteins on platelets and red blood cells after infection with the *S. pneumoniae* $NanA^{-}$ mutant. Data in **a** and **b** are representative of three to five independent experiments comparing at least six mice per group. (**c**) Detection of asialoglycoproteins on platelets after infection with the *S. pneumoniae* $NanA^{-}$ mutant complemented by a functional *nanA* gene in *trans* ($NanA^{T}$). Data are representative of four mice analyzed. (**d**) Platelet abundance in four to eight mice of the indicated genotypes after infection with *S. pneumoniae* WT, *S. pneumoniae* $NanA^{-}$ or *S. pneumoniae* $NanA^{-}$ complemented with $NanA^{T}$ ($NanA^{-}$ + $NanA^{T}$). Similar results were obtained after *S. pneumoniae* WT infection of Asgr-2–deficient mice (data not shown). SPN, *S. pneumoniae*. (**e**) Platelet turnover in uninfected WT mice and in WT or Asgr-1–deficient mice after *S. pneumoniae* WT infection. Each plot includes data from six mice. (**f**) Detection of asialo-vWF by RCA lectin binding and total vWF levels at 0 and 48 h after infection with *S. pneumoniae* WT when bacteremia was $>1 \times 10^{9}$ CFU/ml. Each histogram presents data from four to six mice. All comparative analyses were performed on mice with equivalent levels of bacteremia at each timepoint. ***$P < 0.001$ and **$P < 0.01$. All values are means ± s.e.m.

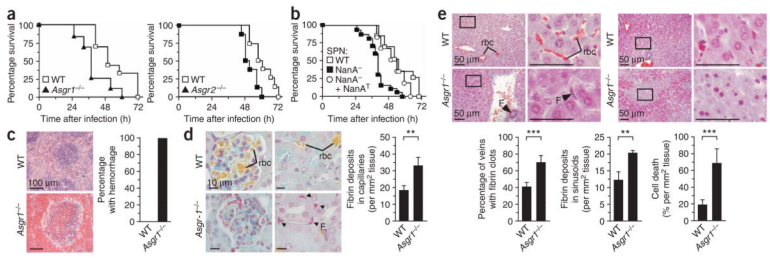

Figure 4.

Extension of lifespan and reduction in coagulopathy by the Ashwell receptor in lethal *S. pneumoniae* infection. (**a**) Survival times of WT and Asgr–deficient mice after infection with a lethal dose of *S. pneumoniae* WT. (**b**) Survival times of WT mice infected with *S. pneumoniae* variants that retain or lack NanA sialidase activity. (**c**–**e**) Tissue histopathology in mice of the indicated genotypes 24 h after infection with *S. pneumoniae* WT. (**c**) Hemorrhage of the spleen with involvement of the lymphoid follicles occurred in all mice lacking Asgr-1. Data are representative of results from eight littermate pairs. (**d**) In the kidney, reduced vascular flow and increased deposition of fibrin (F) were evident in capillaries of the glomeruli and between the tubules. Rbc, red blood cell. (**e**) In the left four images, fibrin deposition was also markedly increased in the veins and sinusoids of the liver in Asgr-1 deficiency (left and center graphs). In the right four images, hepatocyte death was detected by the presence of pyknotic nuclei (right graph). Boxed regions are shown enlarged to the right. Scale bars denote 100 μm (**c**), 10 μm (**d**) and 50 μm (**e**). Images in **c**–**e** are representative of 20–30 randomly selected fields of view used for quantitation. These studies included six or more littermate comparisons of the indicated genotypes infected with equivalent doses of *S. pneumoniae* variants (2×10^5 CFU administered i.p.). All comparisons were performed on mice with equivalent levels of bacteremia. ***$P < 0.001$ and **$P < 0.01$. All values are means ± s.e.m.

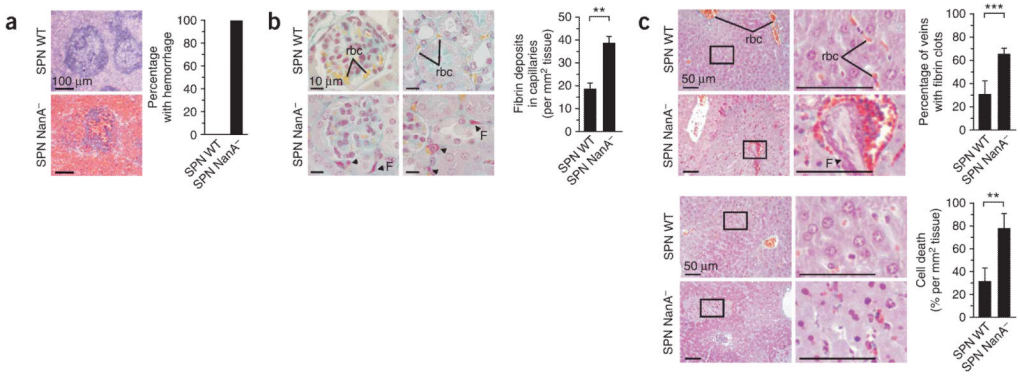

Figure 5.

Increased severity of coagulopathy in sepsis after infection with the *S. pneumoniae* NanA⁻ mutant. Tissue histopathology in WT mice 24 h after infection with *S. pneumoniae* WT (D39) or *S. pneumoniae* NanA⁻. (**a**) Splenic hemorrhage occurred in all mice infected with the *S. pneumoniae* NanA⁻ strain. (**b**) Accumulation of fibrin (F, arrowheads) and impaired vascular flow are evident among capillaries of kidney glomeruli and between tubules. (**c**) Fibrin deposition in liver veins and pyknotic nuclei indicating cell death. Boxed regions are shown enlarged to the right. Scale bars denote 100 μm (**a**), 10 μm (**b**) and 50 μm (**c**). Images are representative of 18–24 randomly selected fields of view used to quantify results. These studies include three to six littermate comparisons of the indicated genotypes infected with equivalent doses of *S. pneumoniae* variants (2×10^5 CFU administered i.p.). All comparisons were performed on mice with equivalent levels of bacteremia. ***$P < 0.001$ and **$P < 0.01$. All values plotted are means ± s.e.m.

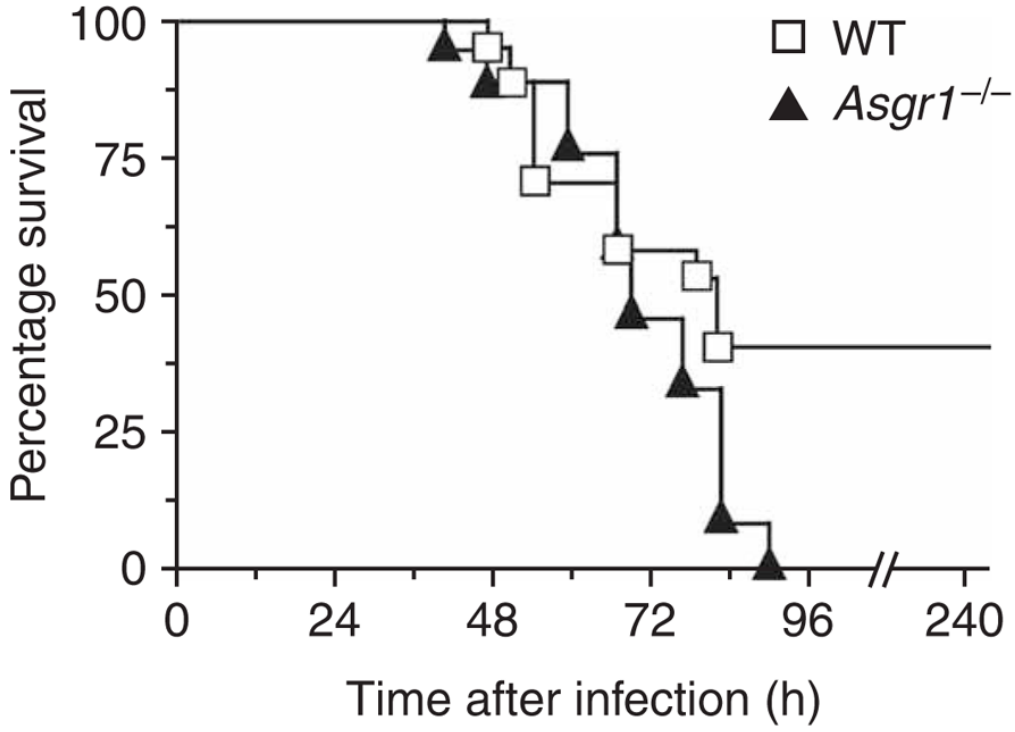

Figure 6.

The Ashwell receptor decreases mortality in *S. pneumoniae* sepsis. None of the 15 Asgr-1–deficient mice survived infection with a low dose of *S. pneumoniae* WT (D39) (1×10^3 CFU administered i.p.). In contrast, 6 of 16 WT littermates survived. This finding was reproduced in three independent experiments with additional cohorts of mice.